



Cite this: DOI: 10.1039/c4dt03152k

Synthesis and characterization of Mg–Al-layered double hydroxides intercalated with cubane-1,4-dicarboxylate anions

Zolfaghar Rezvani,* Farzad Arjomandi Rad and Fatemeh Khodam

In the present work, Mg₂Al-layered double hydroxide (LDH) intercalated with cubane-1,4-dicarboxylate anions was prepared from the reaction of solutions of Mg(II) and Al(III) nitrate salts with an alkaline solution of cubane-1,4-dicarboxylic acid by using the coprecipitation method. The successful preparation of a nanohybrid of cubane-1,4-dicarboxylate(cubane-dc) anions with LDH was confirmed by powder X-ray diffraction, FTIR spectroscopy and thermal gravimetric analysis (TGA). The increase in the basal spacing of LDHs from 8.67 Å to 13.40 Å shows that cubane-dc anions were successfully incorporated into the interlayer space. Thermogravimetric analyses confirm that the thermal stability of the intercalated cubane-dc anions is greater than that of the pure form before intercalation because of host–guest interactions involving hydrogen bonds. The interlayer structure, hydrogen bonding, and subsequent distension of LDH compounds containing cubane-dc anions were shown by molecular simulation. The RDF (radial distribution function), mean square displacement (MSD), and self-diffusion coefficient were calculated using the trajectory files on the basis of molecular dynamics (MD) simulations, and the results indicated that the cubane-dc anions were more stable when intercalated into the LDH layers. A good agreement was obtained between calculated and measured X-ray diffraction patterns and between experimental and calculated basal spacings.

Received 13th October 2014,
Accepted 30th October 2014

DOI: 10.1039/c4dt03152k

www.rsc.org/dalton

Introduction

Layered organic–inorganic hybrid compounds containing biological and biomedical organic anions are a new class of materials and represent a promising advance in the development of multifunctional materials.¹ Recently, much work has focused on the incorporation of various organic anions into layered inorganic host structures for the purpose of improving the thermal and physicochemical properties of these organic anions.² The interlayer spacing of these inorganic host structures are easily expandable due to easy breaking of weak van der Waals or hydrogen bonds.³ Among these layered inorganic host structures, the layered double hydroxides (LDHs) have in particular attracted a lot of attention. Layered double hydroxides consist of positively charged brucite-like layers and negatively charged anions in the interlayer space. These structures can be represented by the general chemical formula $[M_{1-x}^{2+}M_x^{3+}(OH)_2]^{x+}[(A^{n-})_{x/n} \cdot mH_2O]$, where M²⁺ and M³⁺ are di- and trivalent metal cations, respectively, and Aⁿ⁻ represents an exchangeable interlayer anion with a charge of n⁻.⁴ LDH

systems have been widely studied for the purpose of advancing their potential applications, and from a molecular simulations point of view.⁵ Much attention has been paid to the many organic anions incorporated in LDHs. These new materials show new photophysical behaviors and several useful advantages for eco-friendly development. A homogeneous distribution of the organic anions at the molecular level can be facilitated by H-bond and van der Waals interactions and the host–guest interaction based on electrostatic forces in the LDH galleries.⁶

The anions in the interlayer gallery are generally exchangeable, and indeed anion exchange is the most widely used intercalation method. Many different kinds of anions have been successfully intercalated into LDH, including almost all of the common inorganic anions, many organic anions including carboxylates, sulfonates, benzoates, and biomolecular anions such as amino acids, enzymes, DNA and biopolymers.⁷ Investigation of the interlayer arrangement of these compounds is problematic as they usually exhibit a certain degree of disorder, which can prevent adequate structural analysis based on diffraction data only. Combining molecular modeling with experimental measurements, however, can solve this problem.⁵

Because of the considerable increase in computational power over the past decades, molecular dynamics (MD)^{8,9} has

Department of Chemistry, Faculty of Basic Sciences, Azarbaijan Shahid Madani University, Tabriz, Iran. E-mail: zrezvani@azaruniv.ac.ir; Fax: +98 412 432 7541; Tel: +98 412 432 7541

proved to be a useful tool to study molecular self-assembly and this technique can yield detailed atomic-level insight into the three-dimensional structure of the model system. The theoretical simulations provide a complementary and effective method to study and predict the properties and structures of new kinds of functional materials, and some impressive results can be obtained.⁶

Since Eaton and Cole¹⁰ synthesized cubane, there have been numerous reports of syntheses and characterizations of cubane derivatives.^{11–14} Cubane derivatives are widely used as novel organic anions for high-energy explosives, oligomeric compound development and pharmaceutical materials. For example, they are highly lipophilic molecules that bind avidly to the envelope of the AIDS virus. The syntheses and characterizations of nanohybrids of several organic compounds with LDHs have been reported in last decade, but to the best of our knowledge, synthesis, characterization and molecular modeling investigations of LDHs with cubane derivatives have not been reported.

In the present work, the preparation of Mg–Al hydrotalcite intercalated with cubane-1,4 dicarboxylate anions (hereafter abbreviated as cubane-dc) is reported. The product was obtained from the reaction of solutions of Mg(II) and Al(III) salts with an alkaline solution of cubane-1,4-dicarboxylic acid using the coprecipitation method. Since the physicochemical properties of the intercalated material are influenced by the structure of the interlayer space, molecular modeling was used to propose the arrangement of cubane-dc anions in this space.

Experimental

Materials

Cubane-1,4-dicarboxylic acid was prepared by the methods described in the literature.^{10,14,15} All reagents were purchased from the Merck chemical company and used without further purification. NO₃–Mg–Al-LDH was prepared according to the literature.¹

Characterizations

Powder X-ray diffraction patterns (PXRD) of the samples were recorded with a Bruker AXS model D8 Advance diffractometer using Cu-K_α radiation ($\lambda = 1.54 \text{ \AA}$) at 40 kV and 35 mA with 2θ Bragg angles ranging from 2 to 70°. Fourier transform infrared spectra (FT-IR) were recorded in the range of 4000–400 cm⁻¹ using the KBr pellet technique with a Perkin-Elmer spectrophotometer. Thermogravimetric analysis (TGA) was carried out with a Mettler-Toledo TGA 851e apparatus at a heating rate of 10 K min⁻¹ in a nitrogen atmosphere. Scanning electron microscopy (SEM) was used to study the morphology of samples using an ultrahigh resolution FESEM device (model ULTRA55, Carl Zeiss MST AG, Germany). Elemental (C, H, and N) analyses were carried out on a Perkin-Elmer 240B analyzer. Mg and Al contents of the samples were determined by using inductively coupled plasma spectroscopy (Jobin Yvon JY24) after dissolving the samples in nitric acid.

Syntheses of cubane-dc-LDH

A solution containing cubane-1,4-dicarboxylic acid (0.172 g, 0.001 mol) dissolved in NaOH (20 mL, 0.1 M) was slowly added to an aqueous mixed solution (20 mL) of Mg(NO₃)₂·6H₂O (0.5128 g, 0.002 mol) and Al(NO₃)₃·9H₂O (0.375 g, 0.001 mol) with vigorous stirring in a nitrogen atmosphere. The pH of the solution was adjusted to 10.2 by addition of NaOH or HCl dropwise, and the system was heated to reflux at 55 °C for 72 h. The product (cubane-dc-LDH) was centrifuged at a speed of 2000 rpm for 10 min. and the solid obtained was washed thoroughly with deionized water and finally dried at room temperature under vacuum. Anal. calculated for [Mg₄Al₂(OH)₁₂](C₁₀H₆O₄)·2.5H₂O: C, 20.33; H, 3.90; Mg, 16.47; Al, 9.15. Found: C, 19.9; H, 3.98; Mg, 16.0; Al, 8.7.

Molecular modeling

The entire simulation was conducted using the Discover and Forcite modules in the Materials Studio software package.¹⁶ These modules involve a range of well-validated force fields for dynamics simulations, minimization, and analysis searches for periodic solids. It can be desirably employed in studying molecular systems and a variety of materials types. In this article, a perfectly ordered LDH layer model with a hexagonal supercell was made. At first, the DFT method was used to obtain the optimized geometrical configuration for the cubane-dc. After determination of atomic charges, this information was used in the molecular dynamics simulations. The classical force field CVFF was used for the cubane-dc-LDH system.^{17–19} The first step in the simulation was the preparation of the positively charged Mg–Al-LDH layers as the host structure. The host structure was constructed using atomic coordinates from the previously reported X-ray crystal structure of hydrotalcite²⁰ [Mg₄Al₂(OH)₁₂](CO₃)·3H₂O], which was refined in the rhombohedral space group $R\bar{3}m$ with lattice parameters $a = b = 3.054 \text{ \AA}$, $c = 22.81 \text{ \AA}$, $\alpha = \beta = 90^\circ$, and $\gamma = 120^\circ$. In order to study the arrangement of the guests in the interlayer space, a $P1$ superlattice with the dimensions $6a \times 4a \times 3d_{\text{exp}}$ was developed where d_{exp} is d_{003} of cubane-dc-LDH, which was obtained from the X-ray diffraction data. The interlamellar carbonate ions and water molecules were omitted; then a supercell in the form $6a \times 4b \times 1.76c$ was developed with supercell parameters $6a = 18.324 \text{ \AA}$, $4b = 12.216 \text{ \AA}$, $1.76c = 45.625 \text{ \AA}$, $\alpha = \beta = 90^\circ$ and $\gamma = 120^\circ$. In fact, $3d_{003}$ or $3d_{\text{exp}} (= 40.2 \text{ \AA})$ of cubane-dc-LDH is equal to the $1.76c$ of the hydrotalcite structure. The ratio of Mg and Al atoms in the framework was 2 : 1, and the Mg and Al atoms were scattered in every layer arbitrarily. Every hydroxide layer had 8Al³⁺ and 16Mg²⁺ ions, with the latter arranged in such a way that they were not placed in the adjacent octahedra. The cubane-dc anions were randomly located in the interlamellar area of the LDH to neutralize the positive charges for the hybrid system, and then to form a tilted bilayer arrangement. Ten molecules of water were also randomly inserted into the interlamellar area. The atomic charges can be determined from the Mulliken charge, APT charge and ESP charge. In this work, the Mulliken method^{20,21} was used for calculation of

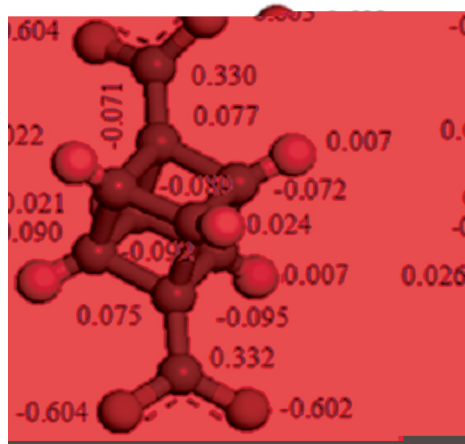


Fig. 1 Mulliken atomic charges of cubane-dc.

atomic charges. Fig. 1 shows the Mulliken charge of the cubane-dc. The Dmol₃ program at the GGA-PBE/DND level optimized the cubane-dc structure. The atomic charges are essential for explaining the cubane-dc structure and the MD properties when cubane-dc anions are placed into the LDH layer.

Layer charges were calculated using the charge equilibration (QEq) method. Since the CVFF force field is relatively accurate for LDH materials,²² the use of this force field improved the LDH partial charges; the partial charges were set to 1.231e or 1.278e for Al, to 0.615e or 0.638e for Mg, to -0.617e or -0.628e or -0.558e for O, and to 0.212e or 0.233e for H.

The minimization was performed using the CVFF force field. The electrostatic energy was obtained using the Ewald summation method²³ and the van der Waals energy was shown using a Lennard-Jones potential.²⁴ The total crystal energy minimization was conducted using a modified Newton method with the following approach: all the layers of the host

were kept as rigid units during the energy minimization period, and the cell parameters c , a , and β were allowed to vary, which enabled the optimization of the arrangement of the host layers; all the atomic positions in the interlayer region were allowed to vary as well.⁶

In this work, we concentrated on the aggregation structure around the anions of cubane-dc intercalated into LDH. Simulations were carried out on structures previously minimized using the smart minimizer procedure of the materials studio software package. The minimized structures were used to set the equilibrium bond lengths and angles. The molecular dynamics simulation was carried out in an NPT statistical ensemble at room temperature (298 K). The time step was 0.5 fs and total time of simulation was 800 ps. Fig. 2 shows that the potential energy reaches a stable equilibrium after 200 ps of simulation time and the last 400 ps were used for further analysis.

Results and discussion

XRD analyses

The XRD patterns for the Mg–Al–NO₃ LDH and the cubane-dc-LDH showed characteristic reflections related to a crystalline layered phase (Fig. 3).^{25,26} In the 2–70° range of 2θ values for the Mg–Al–NO₃ LDHs shown in Fig. 3(a), there are sharp and strong diffraction peaks at low 2θ values, which demonstrate the good crystallinity of LDH nanoparticles.

Mg–Al–NO₃ LDH has a d_{003} basal spacing of 8.67 Å. This spacing, which represents the summation of the thickness of the brucite-like layer (0.48 nm)²⁷ and the gallery height, is a function of the number, size and orientations of the intercalated anions.²⁸

The XRD pattern of the sample with the intercalated cubane-dc anion is shown in Fig. 3(b). During the intercalation of cubane-dc anions, the layers of LDH swell to host the anions, and this expansion is reflected by the 13.40 Å value of

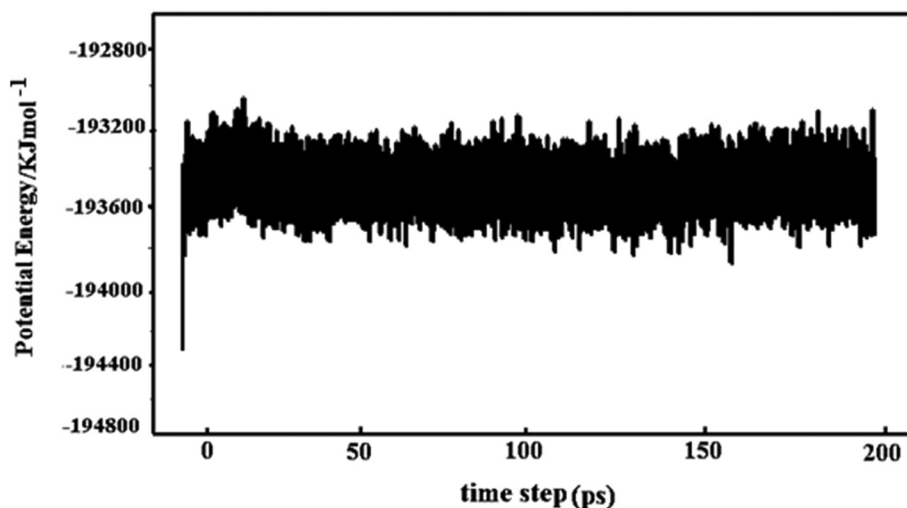


Fig. 2 Time profiles of the total energy (the last 200 ps).

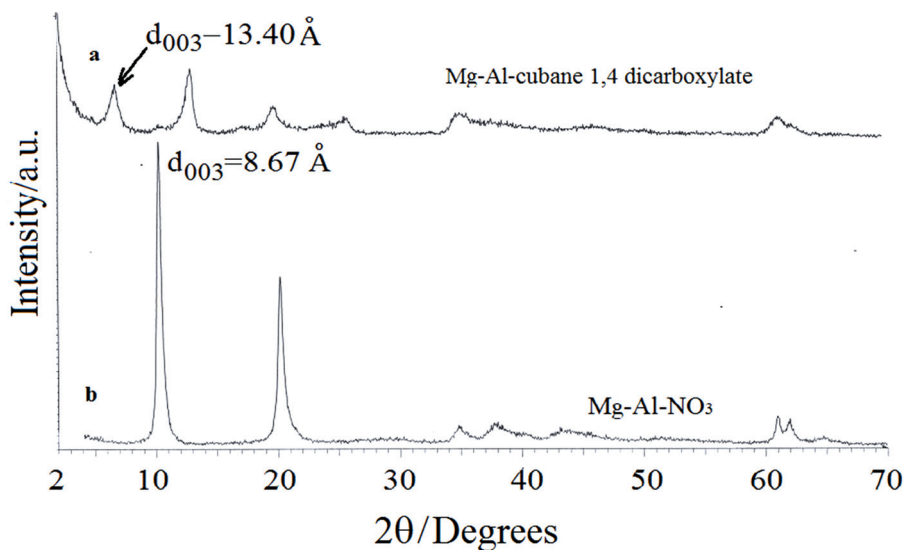


Fig. 3 PXRD patterns of the Mg–Al–NO₃-LDH and Mg–Al-LDH intercalated with cubane-dc.

its d_{003} . This swelling of the layers is due to the intercalation of the cubane-dc anions, and the basal spacing corresponding to diffraction by the (003) planes is much larger than that for the LDH. Taking into account that the thickness of the LDH layer is 4.8 Å and the longitudinal van der Waals radius of the cubane-dc anion is 7.20 Å (determined by the software Chem-Sketch), it was confirmed that cubane-dc anions were successfully intercalated in their anionic form, and that they were arranged as a monolayer within the interlayer.

FTIR spectra

The structure of cubane-dc-LDH was also confirmed by FT-IR spectroscopy. The FT-IR spectra of the cubane-1,4-dicarboxylic

acid and the cubane-dc-LDH are shown in Fig. 4(b and c). The FT-IR spectrum of the Mg–Al–NO₃-LDH is shown in Fig. 4a for comparison.

The spectrum for NO₃-LDH is similar to that reported in the literature.^{29,30} Absorption at 1384 cm⁻¹ can be assigned to the ν_3 vibration of NO₃. A broad, strong absorption band centered at 3451 cm⁻¹ is ascribed to the stretching vibrations of hydroxyl groups and surface and interlayer water molecules,^{31,32} which are found at a lower frequency in LDHs compared to the O–H stretching in free water at 3600 cm⁻¹.³³ This is attributed to the formation of hydrogen bonds between the interlayer water and the different guest anions as well as with the hydroxide groups of the layers. A weaker band at

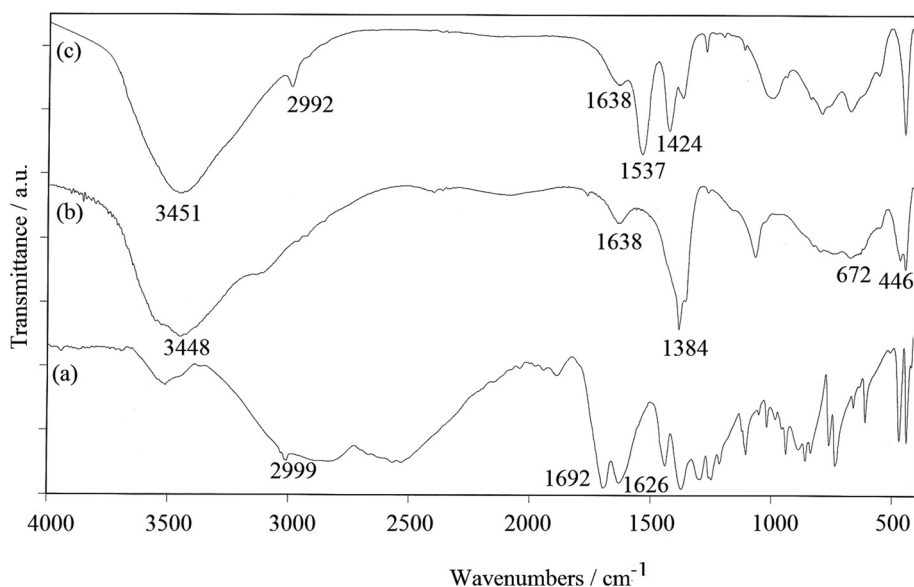


Fig. 4 FT-IR spectra of (a) cubane-1,4-dicarboxylic acid, (b) NO₃-LDH, and (c) cubane-dc-Mg–Al-LDH.

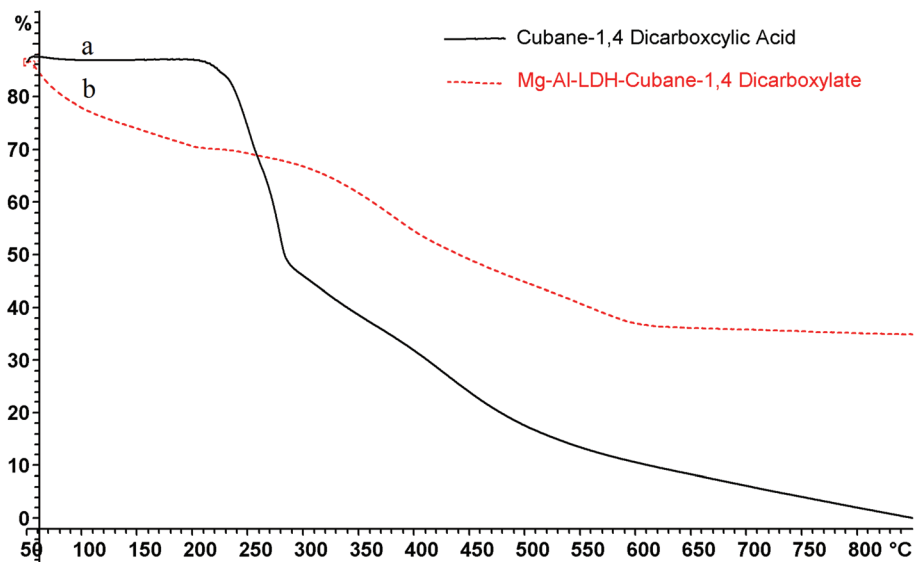


Fig. 5 TGA thermograms of (a) cubane-1,4-dicarboxylic acid and (b) Mg-Al-LDH-cubane-dc.

1638 cm^{-1} was due to the bending mode of water molecules. The bands centered at 446 and 672 cm^{-1} are attributed to Al-O and Mg-O lattice vibrations.²⁹

In the case of pure cubane-1,4-dicarboxylic acid, strong absorption bands centered at 3416 and 3500 cm^{-1} are attributed to the stretching vibrations of OH groups. Furthermore, absorption bands at 1692 and 1626 cm^{-1} are related to the C=O of carboxylate groups. In cubane-dc-LDH, the absence of the NO_3 bands at 1384 cm^{-1} indicates that the preparation process was complete. The band spanning the wavelengths from 1692 to 1626 cm^{-1} due to the COOH group disappears, while the two bands at approximately 1537 and 1422 cm^{-1} due to the anti-symmetric and symmetric stretching vibrations of -COO^- appear and shift to lower wavenumbers, compared to free -COOH in cubane-1,4-dicarboxylic acid, indicating that the intercalation in the interlayer space involves hydrogen bonding, besides the obvious electrostatic attraction between the electropositive cations in the layer and organic anions in the interlayer.^{28,34,35}

Thermal analyses

Thermogravimetric analyses (TGA) are suitable for determining the thermal stabilities of materials, and were thus used to investigate the thermal stabilities of the cubane and the cubane-dc-LDH. The TGA curves are shown in Fig. 5(a, b). In the case of cubane-1,4-dicarboxylic acid (Fig. 5a) there are two distinct steps, one in the temperature range 220–300 °C and the other between 300 and 500 °C, that are attributed to decomposition of cubane-1,4-dicarboxylic acid. The mass loss value of the cubane-1,4-dicarboxylic acid at 850 °C is 87.5%.

Cubane-dc-LDH shows major mass losses in three steps. The first mass loss observed in the 50–200 °C range corresponds to the loss of both adsorbed and interlayer water molecules. A following rapid mass loss between 300 and 400 °C is attributable to the cubane-dc decomposition and dehydroxylation

of the LDH layer. This temperature is higher than the decomposition temperature of pure cubane-1,4-dicarboxylic acid, which occurs at 220 °C. It is confirmed that the thermal stability of intercalated cubane-DC molecule was enhanced by 80 °C. The third mass loss in the temperature range of 400–600 °C is attributed to further dehydroxylation of LDH layers. The mass loss value of the cubane-dc-LDH at 850 °C is 52.17%. Decomposition of cubane-dc-LDH leads to the formation of MgO and Al_2O_3 with an Mg/Al ratio of 2. On the basis of the chemical formula of the cubane-dc-LDH, $[\text{Mg}_4\text{Al}_2(\text{OH})_{12}](\text{C}_{10}\text{H}_6\text{O}_4) \cdot 2.5\text{H}_2\text{O}$, the calculated mass loss is 55.61%. This difference (3.44%) between the calculated and observed mass losses may be due to incomplete oxidation of the carbon.

To further confirm the improvement of thermal stability of cubane-DC anions intercalated into LDH layers, the virgin crystals of this sample were stored at 300 °C for 2 hours, and then an X-ray diffraction pattern and IR spectrum (Fig. 6) were recorded. As seen in Fig. 6(a), the layered structure of the sample is preserved in the annealed sample, but the basal spacing (d_{003}) slightly decreased from 13.40 Å to 12.90 Å, which confirms the loss of water molecules from the interlayer spacing. The FTIR spectrum of the annealed sample (Fig. 6b) shows all vibrations of cubane-dc-LDH, but as can be seen from the spectrum, the intensity of the water molecule bending mode (1638 cm^{-1}) decreased in comparison with the virgin sample (Fig. 5c), which confirms the loss of water molecules from the interlayer spacing.

Results of molecular modeling

The aggregation state of the structure at the microscopic level is a very important factor for determining the macroscopic behavior of the cubane-dc anions intercalated into the layers of

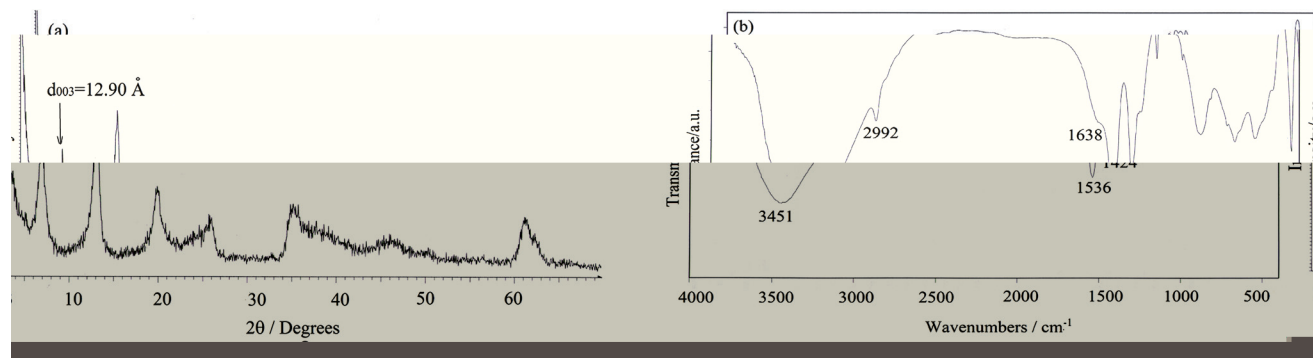


Fig. 6 XRD pattern of cubane-DC -LDH (a), and FTIR spectrum of cubane-dc-LDH (b), annealed at 300 °C for 2 hours.

LDH. MD simulations can show the orientation of the intercalated molecules at the molecular level and lead to a determination of the arrangement of the guest cubane-dc anions in the interlayer region. Fig. 7(a) and (b) show snapshots of equilibrium structures of the cubane-dc-LDH system before and after MD simulation. Note that the cubane-dc anions and water molecules were, prior to the simulation, placed randomly in the interlayer space of the LDH. Through analyzing the trajectories, the equilibration of the simulation systems reveals the arrangement of cubane-dc anions. Molecular dynamic calculations reveal that the long axis of the cubane-dc anions in the interlayer space is tilted approximately 54° from a perpendicular orientation to the LDH layer. These calculations also showed that guest anions are not randomly distributed in the interlayer space but they have a tendency to assemble in rows, albeit with a certain level of disorder.

The end-group-water interaction can be described by partial radial distribution functions (RDFs), which indicate how many atoms of type A are on average a distance r from an atom of type B.⁶ Relevant RDFs of water molecules with cubane-dc anion end-groups were calculate over the last 800 ps of the molecular dynamics calculation (Fig. 8). As can be seen from

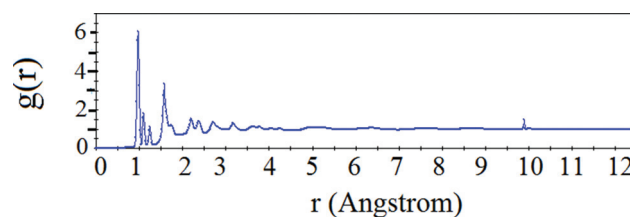


Fig. 8 RDFs between end-group and water.

Fig. 8, the water molecules are dispersed in the interlayers of LDH around the end-groups, and can be divided into two main shells, which are respectively located about 0.97 Å and 1.57 Å from the cubane-dc anion end-groups. Most of the water molecules form close contacts with OH^- of the LDH layer and the $-\text{COO}^-$ groups of the guest anions. Fig. 9 is a schematic of the H-bond structure between the end-groups and the water molecules, which shows that most of the hydrogen bonds in the hybrid systems are made between O atoms of end-groups and OH^- in the LDH layers, and then with the water molecules.

To study the effective delivery of cubane-dc anions, which use LDH as carriers, we have obtained the mean square

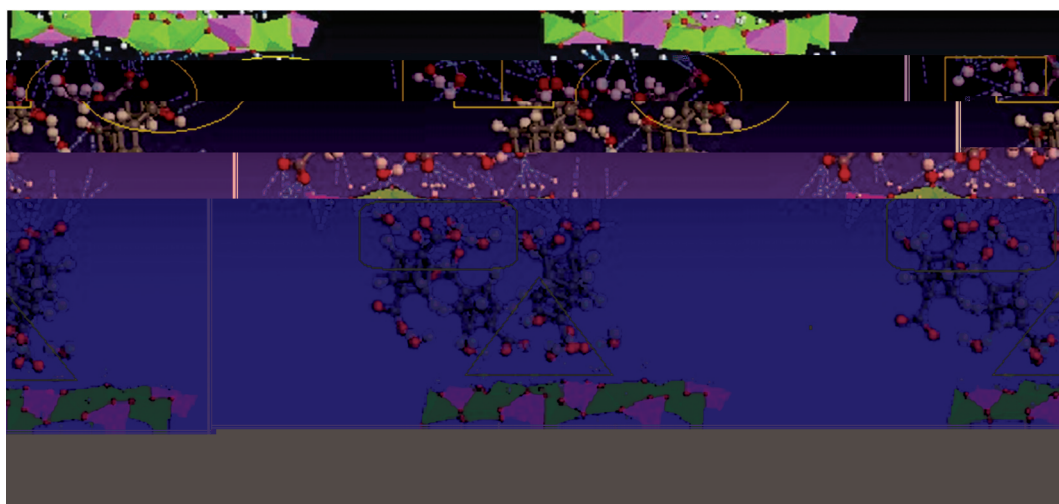


Fig. 7 Snapshots of the equilibrium structures for cubane-dc-LDH (a) before and (b) after MD simulation.



Fig. 9 Hydrogen bonds in the hybrid system.

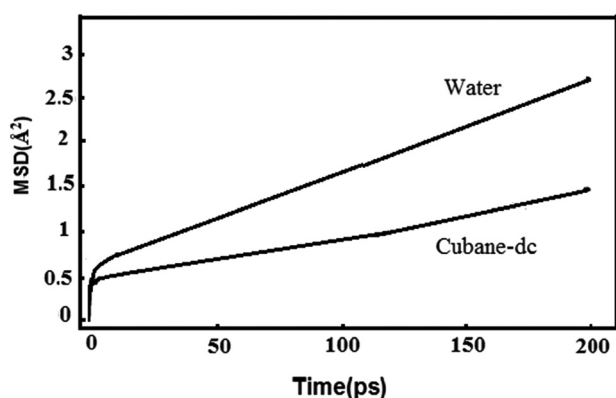


Fig. 10 Comparison of the calculated MSDs for cubane-dc and water molecules.

displacements (MSDs) of the cubane-dc and water molecules from the last 200 ps MD trajectory (time step = 0.5 fs and total time of simulation = 400 ps). The analysis of the MSD yields important information about the stability of the cubane-dc-LDH system. The MSDs of the two different molecules in the 200 ps of the trajectory are shown in Fig. 10, in which the slopes of the MSD-versus-time curves are consistent with the system achieving equilibrium. The MSD was obtained from eqn (1),⁶

$$\text{MSD}(t) = \left\langle \frac{1}{N} \sum_{i=1}^n [r_i(t) - r_i(0)]^2 \right\rangle \quad (1)$$

where N is the number of target molecules and $r_i(t)$ is the location of molecule i at time t . The diffusion coefficient (D) can then be obtained by using the famous Einstein relation (eqn (2))³⁶

$$D\alpha = \frac{1}{2dN\alpha} \lim_{t \rightarrow \infty} \frac{d}{dt} \langle [r_i(t) - r_i(0)]^2 \rangle \quad (2)$$

where d is the system dimensionality, and $r_i(t)$ and $r_i(0)$ are the coordinates of the center of mass of the i th cubane-dc and

water molecules at the times t and 0, respectively. Once the MSDs as a function of time are calculated, it is then possible to calculate the self-diffusion coefficient. Eqn (1) implies that MSD exhibits linear dependence on time, and the self-diffusion coefficient is just the slope of the line. For short time periods, the MSD dependence on time is clearly not linear, but it does become linear for longer periods of time. Diffusion coefficients should be determined only using data in the region where MSD depends linearly on time, and by using linear regression.³⁷ Fig. 10 indicates the obtained MSD for the dispersed water molecules in comparison with the obtained MSD for the anions of cubane-dc. According to the MSD curves, the self-diffusion coefficients of water and cubane-dc were calculated to be $(1.647 \pm 0.05) \times 10^{-7} \text{ cm}^2 \text{ s}^{-1}$ and $(6.543 \pm 0.05) \times 10^{-8} \text{ cm}^2 \text{ s}^{-1}$ respectively. Based on this result, the self-diffusion coefficient of cubane-dc is significantly lower than that of the water molecule. From the above-mentioned analysis we can conclude that the cubane-dc anions are restricted to the layers of LDH and the cubane-dc anions are more stable when intercalated into these layers. The stability is highly important since it can overcome the thermal instability when cubane-1,4-dicarboxylic acid is used alone.²⁷

Comparison of experimental and calculated XRD

The orientation of cubane-dc anions within the interlayer space depends on the space available to the guest anions in the interlayer region. On the basis of the d_{003} value of cubane-dc-LDH (measured by X-ray diffraction), the space available to the cubane-dc anions in the interlayer space is 8.6 Å, which can be approximately calculated by subtracting the 4.8 Å thickness of the layer from the 13.4 Å interlayer spacing. According to the longitudinal van der Waals radius of the cubane-dc anion (7.20 Å), there is enough vacant space available for guest anions. On the other hand, the orientation of guest anions depends on the interactions of guest anions with LDH layers and interlayer water molecules, as well as on interactions among guest anions.

Experimental XRD results combined with molecular simulations can determine the potential orientations of the cubane-dc guest anions in the interlayer space. The water content of the interlayer space and the position of the interlayer water as well as the orientation of guest anions (cubane-dc) strongly influence the X-ray diffraction patterns. By using molecular modeling and molecular dynamic calculations, the water molecules and guest anions were arranged within the interlayer so that the calculated XRD pattern agrees with the measured one. Fig. 11 shows the calculated and experimental XRD patterns of cubane-dc-LDH.

The experimental XRD pattern shows that the peak maxima of d_{003} , d_{006} and d_{009} were observed at 13.40, 6.92 and 4.52 Å, respectively, while the calculated XRD pattern show them to be at 13.39, 6.69 and 4.46 Å, respectively. Note the particularly good agreement between the calculated and experimental d_{003}

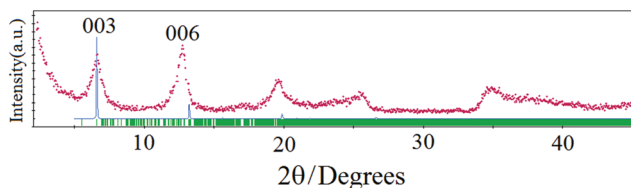


Fig. 11 The calculated (solid) and experimental (dotted) x-ray diffraction patterns.

spacings. The slightly lower value for the calculated d_{006} spacing compared to that of the experimental d_{006} may be related to the effect of crystal size on peak broadening as well as to the high disorder of guests in the structural model, which is not taken into account in the software.⁵

As can be seen from Fig. 11, the intensities of the experimentally determined (003) and (006) peaks are inverted compared to those in the calculated XRD pattern. This observation is due to the roughness of the surface of the experimental sample, which is not considered in the software.⁵ This effect is common when the electron density of the interlayer space is comparable to or higher than that of the brucite sheet.

Comparison with terephthalate-intercalated Mg–Al-LDH

G. Lagaly *et al.* reported the syntheses, characterizations and basal spacings of several dicarboxylate-intercalated-Mg–Al layered double hydroxides.³⁸ Among the reported cases, the size of the terephthalate dianions is very close to that of the cubane-dc anions. The distances between carboxylate end-groups in the terephthalate and cubane-dc are 7.1 Å and 7.2 Å, respectively. The basal spacing (d_{003}) of terephthalate-Mg–Al-LDH hybrid is 14.3 Å. This value is significantly higher (by 0.9 Å) than the 13.40 Å basal spacing of the cubane-dc-Mg–Al-LDH nanohybrid. This difference may be related to the tilted arrangement of cubane-dc dianions in the interlayer region.

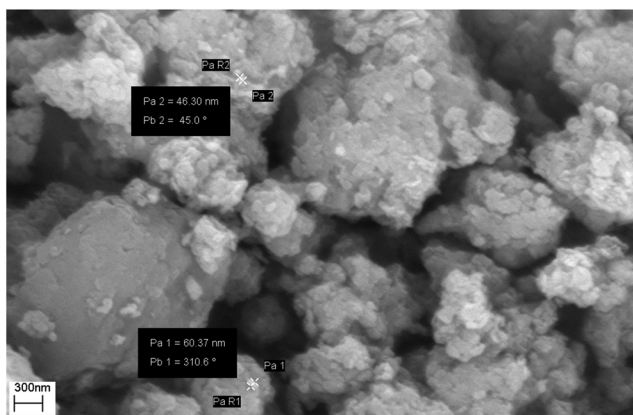


Fig. 12 SEM image of cubane-dc-LDH.

SEM

A scanning electron microscopy (SEM) image of a cubane-dc-LDH nanohybrid is depicted in Fig. 12. The irregular sheet-like character of cubane-dc-LDH nanohybrid can be clearly seen in this figure. In fact, cubane-dc-LDH is composed of aggregates of irregular sheet-like nanoparticles with sheet thicknesses in the range of 40–60 nm. The broadening of the XRD pattern of cubane-dc-LDH (Fig. 11) is due to the nanosize of the particles.

Conclusions

The synthesis and characterization of Mg–Al hydrotalcite intercalated with cubane-dc anions are reported. The successful intercalation of cubane-1,4-dicarboxylate anions into the interlayer space of LDH was confirmed by powder X-ray diffraction, FTIR spectroscopy and thermal gravimetric analysis (TGA). During the intercalation of cubane-dc anions, the layers of LDH swell to host the anions, and this expansion is reflected by the value of d_{003} . A molecular dynamics simulation was used to investigate the arrangement of the guest anions within the interlayer space of LDH. The results show that the long axis of cubane-dc anions is tilted approximately 54° from the perpendicular orientation to the LDH layer. Based on RDF results, the water molecules are dispersed in the interlayers as two main shells, which are positioned about 0.97 Å and 1.57 Å from the cubane-dc anion end-group. The dynamical properties such as mean-square displacements (MSD) and thus self-diffusion coefficients (D) were also analyzed for intercalated cubane-dc anions and water molecules. The results of the MD showed that the cubane-dc anions were more stable when intercalated into layers of LDH.

Acknowledgements

We are grateful for the support from Azarbaijan Shahid Madani University. We also thank the research laboratory of Dr M. Mahkam (Azarbaijan Shahid Madani University) for preparation of cubane-1,4-dicarboxylic acid.

Notes and references

- 1 S. P. Lonkar, B. Kutlu, A. Leuteritz and G. Heinrich, *Appl. Clay Sci.*, 2013, **71**, 8.
- 2 T. Zehi, M. Wahab, H. J. Mögel and P. Schiller, *Langmuir*, 2006, **22**, 2523.
- 3 A. J. Howes and C. J. Radke, *Langmuir*, 2007, **23**, 1835.
- 4 V. Rives, *Layered Double Hydroxides: Present and Future*, Nova Science Publishers, 2001, p. 1.
- 5 P. Kovar, K. Melanova, V. Zima, L. Benes and P. C. Apkova, *J. Colloid Interface Sci.*, 2008, **319**, 19.
- 6 K. Lv, H. Kang, H. Zhang and S. Yuan, *Colloids Surf., A*, 2012, **402**, 108.

- 7 H. Zhang, Z. P. Xu, G. Q. Lu and S. C. Smith, *J. Phys. Chem., C*, 2009, **113**, 559.
- 8 N. R. Tummala and A. Striolo, *J. Phys. Chem. B*, 2008, **112**, 1987.
- 9 E. Khurana, S. O. Nielsen and M. L. Klein, *J. Phys. Chem. B*, 2006, **110**, 22136.
- 10 P. E. Eaton and T. W. Cole, *J. Am. Chem. Soc.*, 1964, **86**, 962.
- 11 G. W. Griffin and A. P. Marchand, *Chem. Rev.*, 1989, **89**, 997.
- 12 A. P. Marchand, *Chem. Rev.*, 1989, **89**, 1011.
- 13 P. E. Eaton, *Angew. Chem., Int. Ed. Engl.*, 1992, **32**, 1421.
- 14 K. Hassenruck, J. G. Radziszewski, V. Balaji, G. S. Murthy, A. J. Mckinley, D. E. David, V. N. Lynch, H. D. Martin and J. Michl, *J. Am. Chem. Soc.*, 1990, **112**, 873.
- 15 N. B. Chapman, J. M. Key and K. J. Toyne, *J. Org. Chem.*, 1970, **35**, 3860.
- 16 *Discover, User Guide, Accelrys, Molecular Simulations Inc*, San Diego, USA, 1996.
- 17 J. L. Zhang, M. Zhang, J. J. Wan and W. Li, *J. Phys. Chem. B*, 2008, **112**, 36.
- 18 V. Varshney, S. S. Patnaik, A. K. Roy and B. L. Farmer, *J. Phys. Chem. C*, 2010, **114**, 16223.
- 19 G. Raffaini and F. Ganazzoli, *J. Phys. Chem. B*, 2010, **114**, 7133.
- 20 M. Bellotto, B. Rebours, O. Clauses, J. Lynch, D. Bazin and E. Elkaïm, *J. Phys. Chem.*, 1996, **100**, 8527.
- 21 X. M. Liu, S. J. Zhang, G. H. Zhou, G. W. Wu, X. L. Yuan and X. Q. Yao, *J. Phys. Chem. B*, 2006, **110**, 12062.
- 22 S. T. Zhang, H. Yan, M. Wei, D. G. Evans and X. Duan, *J. Phys. Chem. C*, 2012, **116**, 3421.
- 23 N. Karasawa and W. A. Goddard, *J. Phys. Chem.*, 1989, **93**, 7320.
- 24 J. E. Lennard-Jones, *Proc. R. Soc. London, Ser. A*, 1925, **109**, 584.
- 25 A. N. Ay, B. Z. Karan and A. Temel, *Microporous Mesoporous Mater.*, 2007, **98**, 1.
- 26 P. Kustrowski, D. Sulkowska, L. Chmielarz, A. Rafalska-Lasocha, B. Dudek and R. Dziembaj, *Microporous Mesoporous Mater.*, 2005, **78**, 11.
- 27 C. Li, G. Wang, D. G. Evans and X. Duan, *J. Solid State Chem.*, 2004, **177**, 4569.
- 28 J. T. Klopprogge, L. Hickey and J. L. Frost, *Appl. Clay Sci.*, 2001, **18**, 37.
- 29 M. Wei, X. Xu, J. He, Q. Yuan, G. Rao, D. G. Evans, M. Pu and L. Yang, *J. Phys. Chem. Solids*, 2006, **67**, 1469.
- 30 F. Cavani, F. Trifiro and A. Vaccari, *Catal. Today*, 1991, **11**, 173.
- 31 K. Nakamoto, *Infrared and Raman Spectra of Inorganic and Coordination Compounds*, Wiley, New York, 5th edn, 1997.
- 32 S. J. Santosa, E. S. Kunarti and E. Karmanto, *Appl. Surf. Sci.*, 2008, **254**, 7612.
- 33 H. Gunzler and H. U. Gremlich, *IR Spectroscopy: An Introduction*, Wiley-VCH, Weinheim, 2002.
- 34 H. Zhang, K. Zou, S. Guo and X. Duan, *J. Solid State Chem.*, 2006, **179**, 1792.
- 35 *Layered Double Hydroxides*, ed. X. Duan and D. G. Evans, Springer-Verlag, Berlin/Heidelberg, 2006.
- 36 M. P. Allen and D. J. Tildesley, *Computer Simulation of Liquid*, Oxford Science Publications, Oxford, 1987.
- 37 D. Frenkel and B. Smit, *Understanding Molecular Simulation: From Algorithms to Applications*, Academic Press, San Diego, 2th edn, 2002.
- 38 M. Meyn, K. Beneke and G. Lagaly, *Inorg. Chem.*, 1990, **29**, 5201.